Belgiovine *et al.*
Journal of Translational Medicine (2025) 23:454
https://doi.org/10.1186/s12967-025-06407-4

Journal of Translational Medicine

RESEARCH

Open Access

Malignant mesothelioma-associated inflammatory microenvironment promotes tumor progression via GPNMB

Cristina Belgiovine[1,11*], Elisabeth Digifico[1], Marco Erreni[2,3], Anna Rita Putignano[1], Laura Mannarino[2,4], Sonia Valentino[1], Fabio Grizzi[1], Fabio Pasqualini[1,2], Camilla Recordati[5,6], Luca Bertola[5,6], Paolo Zucali[2,7], Daniela Pistillo[8], Valentina Paleari[8], Alberto Mantovani[1,2,9], Maurizio D'Incalci[2,4], Federica Marchesi[1,10] and Paola Allavena[1]

Abstract

Background Tumor-Associated Macrophages (TAMs) are the main immune component of the tumor stroma with heterogeneous functional activities, predominantly suppressing the immune response and promoting tumor progression, also via secretion of different factors. Among these, GPNMB (Glycoprotein non-metastatic B) is usually associated with disease progression in several tumor types. Malignant pleural mesothelioma (MPM) a severe neoplasia with poor prognosis, is characterized by an abundancy of TAMs, testifying the presence of a long-lasting inflammation which is pathogenetic of the disease. However, the role of GPNMB in MPM is unclear.

Methods Clinical samples from patients with MPM were used to measure RNA and protein levels of GPNMB. The functional role of GPNMB in vivo was studied in an orthotopic mouse model of mesothelioma using the murine cell lines AB1 and AB22. Experiments included in vivo tumor growth in wild type and in GPNMB-deficient mice and blocking of GPNMB-induced signaling with anti-CD44 antibodies.

Results We show that in human and murine MPM tissues the protein GPNMB is mainly produced by infiltrating TAMs. *Gpnmb* RNA levels in MPM patients from TCGA are significantly associated with lower survival. Using an orthotopic mouse model of mesothelioma we observed that in GPNMB-defective mice (DBA2/J mice) unable to produce the protein, tumors formed by AB1 and AB22 mesothelioma cells grow significantly less than in GPNMB-proficient mice (DBA2/J-Gpnmb+ mice), indicating that host GPNMB is involved in tumor progression. Likewise, the ectopic expression of GPNMB in AB1 and AB22 cells causes an acceleration of tumor growth in vivo, significantly different compared to mock-transduced cells. Treatment of tumor-bearing mice with blocking anti-CD44 (a major receptor for GPNMB) results in a significant reduction of tumor growth.

Conclusions Overall, these results indicate that the protein GPNMB, a product and marker gene of TAMs, is a driver of mesothelioma progression and may constitute a promising therapeutic target.

Keywords Malignant mesothelioma, GPNMB, Tumor-associated macrophages, Anti-CD44, Orthotopic model

*Correspondence:
Cristina Belgiovine
Cristina.belgiovine@unipv.it
Full list of author information is available at the end of the article

Introduction

In the tumor microenvironment (TME) myeloid cells, and in particular Tumor-Associated Macrophages (TAMs), are immunosuppressive and have several protumoral functions, thus limiting anti-tumor immunity and an efficient response to treatments [1–7]. Among the various protumor mediators produced by TAMs, we and others have reported that tumor-cocultured macrophages produce the Glycoprotein non-metastatic B (GPNMB), also named Osteoactivin or DC-HIL, and release the shed soluble protein [8–10]. GPNMB is a highly glycosylated protein localized in the cell membrane and in the phagosome compartment. The transmembrane form can be cleaved by proteases to generate the soluble extra-cellular domain containing a heparin binding site and an RGD motif binding to integrins. GPNMB also binds to CD44 and to other receptors: EGFR and VEGFR [11–15]. In homeostasis, GPNMB is expressed in several tissues, primarily in the bone, by osteoblasts and osteoclasts, by melanocytes in the skin, in leukocytes of the myeloid lineage, including macrophages, dendritic cells and microglia, and in vascular endothelial cells [12, 13, 15, 16]. GPNMB has various functional roles, from modulation of crucial cell functions (adhesion, migration, differentiation and growth) to negative regulation of the inflammatory responses and stimulation of repair processes in injured tissues [17–22]. In the immune system, GPNMB shows relevant inhibitory effects: DCs and MDSC express GPNMB that binds to syndecan-4 on T cells and suppresses their activation and tissue infiltration by retaining T lymphocytes adherent to endothelial cells [10, 23–25]. The anti-inflammatory role of GPNMB was shown initially in LPS-stimulated macrophages with inhibition of inflammatory cytokine production [21] and further demonstrated in conditions of chronic inflammation such as colitis [26, 27], renal diseases [28, 29], neurodegenerative diseases [30–33], metabolic disorders [18, 34, 35] and autoimmune diseases [36].

In the last decade, attention to GPNMB has considerably increased and several studies have associated its expression and function with cancer. High levels of GPNMB have been found in several cancer types: melanoma, glioblastoma, breast cancer (including triple-negative neoplasia), lung cancer and cholangiocarcinoma [37–40]. Although this protein was initially identified in low metastatic melanoma cell lines [11], it is now clear that its expression in tumors is more frequently associated with malignant progression [39, 41–43].

Important functional activities of GPNMB affect cancer progression, including enhanced tumor cell growth in vitro and in vivo; activation of MMPs in cancer cells, induced by upregulated GPNMB, promotes tumor invasion, migration and metastases [44–48]. In addition, the soluble form of GPNMB showed angiogenic properties, stimulating endothelial cell migration and activation of the FGFR1 [14, 44, 49].

We and others have reported that in tumor-specific knock-down and overexpression models, GPNMB not only enhances tumor growth but also promotes stem-like properties in cancer cells [9, 15, 50, 51].

The immunosuppressive activity of GPNMB, namely inhibition of T cell activation, is also relevant in the context of the TME and anti-tumor immune responses [24, 52, 53].

Several studies reported that high expression of GPNMB can be a poor prognostic factor in some cancers and a mechanism of resistance to immunotherapy [23, 40, 54–58]. In human hepatocellular carcinoma, glioma, and colorectal liver metastases, GPNMB is secreted specifically by tumor-infiltrating myeloid cells. Furthermore, the density of macrophages expressing GPNMB was associated with poorer survival of patients [46, 59–61]. Although its pro-tumorigenic role has been reported in several types of cancer, little is known about the involvement of GPNMB in the progression of malignant pleural mesothelioma (MPM), a disease mostly linked to long-lasting chronic inflammation induced by the inhalation of non-degradable asbestos fibres. MPM is a very aggressive tumor usually non responsive to current treatments, including immunotherapy [62–68]. Acquiring more knowledge on the biological regulation of tumor progression is pivotal to identifying novel therapeutic targets. Here, we show that GPNMB in human MPM is mainly expressed by TAMs. Lack of host GPNMB in *Gpnmb*-mutant mice showed significantly reduced tumor growth in an orthotopic murine model of MPM, while ectopic expression of GPNMB in mesothelioma cells dramatically increased disease progression. These results indicate that GPNMB has a pro-tumoral role in MPM and can be exploited as a therapeutic target.

Materials and methods

Mesothelioma patients

Tumor samples were obtained from 28 patients with pathologically confirmed pleural malignant mesothelioma (MPM) admitted at the IRCCS Humanitas Research Hospital (Rozzano, Milano, Italy). Biological samples were collected before start of therapy and immediately frozen or formalin-fixed and stored in the Institutional Biobank. Plasma samples were collected from 72 chemo-naive MPM patients admitted to Humanitas Hospital. Plasma samples from 86 normal healthy volunteers were also studied as controls. All the experiments were conducted after approval by the Ethic Committee of the Humanitas Research Hospital (protocol code 306/18). Written informed consent was obtained from each

patient before entering the study. Recommendations of the Declaration of Helsinki were followed.

ELISA quantification of GPNMB

To quantify the production of human/murine GPNMB, in cell supernatants or plasma samples from human subjects, the commercial ELISA kits (R&D Systems DY2330 for mice, DY2550 for human) were used, according to the manufacturer's instructions. Data were analysed with SoftMax Pro 5.3 software.

Analysis of TCGA MESO RNA-seq data

The gene expression quantification (STAR Counts) and the clinical information were downloaded from GDC using the R package TCGAbiolinks (v2.25.3, R v4.1.1). (*GDCquery(project = "TCGA-MESO", data.category = "Transcriptome Profiling", data.type = "Gene Expression Quantification", experimental.strategy = "RNA-Seq", workflow.type = "STAR – Counts"*) [69, 70]. The RNA counts were filtered and normalized using DESeq2 (v1.34) [71]. Variance stabilizing transformed (VST) data were used as input for survival analysis.

The surv_cutpoint function of the survminer R package (v0.4.9) (https://CRAN.R-project.org/package=survminer) was used to categorize the TCGA patients into low and high expression groups by determining the optimal cutpoint for each variable (GPNMB, CD44, IL33) related to the outcome (overall survival in our case) based on the maximally selected rank statistics from the 'maxstat' R package (v0.7). The optimal cutpoint for each gene using the "maxstat" method was found respectively at 13.53 (GPNMB), 13.45 (CD44), 8.99 (IL33). Survival analysis on the high and low expressing groups was performed using survival R package (v3.4) [72] and the Kaplan–Meier curves for both groups were visualized with the ggsurvplot function of the survminer package. The statistical significance of survival difference between the two groups of patients was assessed using the log-rank test (p-value lower than 0.05 was considered significant).

Established human and murine mesothelioma cell lines

The human mesothelioma cell lines used in this study were derived from primary tumor samples of patients isolated from pleural effusion and/or lavage of the thoracic cavity and established in vitro, as described [73].

The murine mesothelioma cell lines AB1 (sarcomatoid histology) and AB22 (epithelioid histology), were generated in BALB/c mice upon intraperitoneal injection of crocidolite asbestos fibers and deposited in the Australian cell bank [74]. Luciferase-expressing AB1 and AB22 cells were kindly provided by Prof. M. Bianchi, San Raffaele Scientific Institute, Milan, Italy [75]. Cell lines were cultured in RPMI 1640 (Lonza) supplemented with- 10% FBS (Sigma), 2mM L-glutamine, 100 U/mL penicillin and 100 mg/mL streptomycin (Life Technologies Inc.) at 37 °C and 5% CO2. All cell types were routinely checked for Mycoplasma contamination.

To overexpress the Gpnmb gene, AB1 and AB22 cells were stably transduced with a lentiviral plasmid that constitutively expressing endogenous GPNMB. The murine coding sequence of Gpnmb was cloned in frame with the fluorescent reporter mCherry under the CMV promoter in a lentiviral vector (GPNMB-mCherry pRRL-Sin), and an empty vector containing only mCherry (mCherry pRRL-Sin) was used as a control. Transduction of the AB1 and AB22 cell lines was performed by generating viral particles in HEK293T cells transfected with Lipofectamine 2000 (Thermo Fisher Scientific) according to the manufacturer's instructions. The generated cell lines were expanded 24 h after the last transduction, and GPNMB expression was then assessed by flow cytometry and ELISA.

In vitro colony and tumor spheroid assay

Proliferation of Mock and GPNMB-transduced murine mesothelioma cell lines was quantified by staining with Crystal violet after 1 week; colonies were dissolved in pure DMSO and optical density measured by spectrophotomer at 590 nm. For the spheroid formation assay, Mock and GPNMB-transduced murine mesothelioma cells were cultured in Iscove's medium (Lonza) supplemented with 100 U/mL penicillin and 100 µg/mL streptomycin and the following growth factors: mEGF (PeproTech, 20 ng/mL), mFGF (PeproTech, 20 ng/mL), B27 (Gibco, cat. no. 12587-010), and N2 (Gibco, cat. no. 17502-048). Spheroids were cultured for 1 week and then sphere were disaggregated by pipetting, cells counted and subjected to flow cytometry for stem cell marker analysis with the following antibodies: anti-CD117-PECy7 and anti-CD199-PE (Invitrogen).

The labeled cells were fixed in PBS + 1% formalin. The data were acquired with a FACS Fortessa instrument (BD Biosciences) and analysed by FACS Diva and FlowJo software version 6.1.1 (BD Biosciences).

Preparation of monocyte-derived macrophages and culture with tumor-conditioned medium (CM)

Human monocytes were obtained from normal donor buffy coats by two-step gradient centrifugation. PBMCs were isolated by centrifugation with a Histopaque-1077 gradient (Sigma); monocytes were separated by centrifugation with a Percoll density gradient (GE Healthcare) as described [9].

Purified human monocytes were plated at 10^6/mL in RPMI 1640 + 5% FBS with 25 ng/mL hr M-CSF to induce

macrophage differentiation and 30% tumor CM. Cultures were incubated for 5 days.

Tumor-CM was prepared by growing tumor cells to 90% confluence in fresh RPMI medium without FBS for 24 h; the CM was collected, passed through 0.2 mm filters and stored at − 20 °C.

In vivo experiments in mice

Mice were used in compliance with national (D.L. N. 26, G.U. March 4, 2014) and international law and policies (EEC Council Directive 2010/63/EU, OJ L 276/33, 22-09-2010; National Institutes of Health Guide for the Care and Use of Laboratory Animals, (authorization N° 296/2020-PR), and US National Research Council, 2011). BALB/c mice 8 weeks-old were purchased from Charles River. The procedures for the syngeneic orthotopic mouse model have been previously described [76]. Briefly, mice were anesthetized with ketamine/xylazine and positioned on left lateral decubitus. AB1 and AB22 MPM cells (5×10^4 cells in 50 µl saline solution) were injected intra-thoracically between the third and the fourth costal space. Tumor growth quantification was performed by in vivo imaging over time. Mice were i.p. injected with D-Luciferin (XenoLight D-LuciferinK + Salt, PerkinElmer; 150 mg Luciferin/kg body weight). Ten minutes after D-Luciferin injection, the bioluminescent signal was acquired using the IVIS Lumina III system (Perkin Elmer). During the acquisition procedure, mice were anesthetized with Isoflurane (XGI-8 Gas anaesthesia system, Perkin Elmer). Data were analysed with Living image 4.3.1 by designing a ROI on the thoracic area of each mouse and expressed as average radiance or calculated as fold increase over the previous quantification days. Tumor load was also calculated by classical histopathology. To block the CD44 receptor, mice were treated intra-peritoneally with anti-CD44 mAb (BioXcell, BE0039,10 mg/kg, clone IM7), or an irrelevant antibody at days 8, 11, 14, 17 and 20 post tumor injection.

Immunohistochemistry and RNAScope

Paraffin-embedded human tissues were retrieved from the pathological archive; 3-µm sections were stained with primary antibodies: hGPNMB (BAF2330,) or hCD206 (AF2534) all from R&D System. RNAscope ISH technology was performed with GPNMB RNA-specific probes (RNAscope™ Probe-Hs-GPNMB-C3, ACD, Biotechne), and anti-hCD68 (MAB20401, R&D System), following the manufacturer instructions. For murine tumor tissues, 3-µm sections of paraffin-embedded lungs were stained with the following primary antibodies raised against Iba1 (019–19741, Wako Chemicals), CD3 (MCA1477, Clone: CD3-12, Biorad), CD8 (4SM15; 14–0808-82, eBioscience), GPNMB (BAF2330, R&D System), CD31 (AF3628, R&D System) and F4-80 (MF48000, Invitrogen). Slides were subsequently digitized using the dotSlide virtual microscopy system (Olympus, Italy). Images were then processed in ImageJ software (http://rsb.info.nih.gov/ij/) to calculate the positive area/total area ratio expressed in percentage.

Crossing of BALB/c X DBA/2J mice

The murine AB1 and AB22 MPM cells are of BALB/c background. Therefore, to perform experiments in mice lacking the *Gpnmb* gene, we crossed DBA/2J mice (Jackson Lab. Strain #:000671) lacking a functional *Gpnmb* gene [77], with BALB/c mice (Scheme depicted in Suppl. Figure 3). The resulting offspring: BALB/c X DBA/2J mice were named GPNMB KO mice and were verified to accept the transplanted AB1 and AB22 cells. Luckily, the BALB/c and DBA/2J strains have a high immunological match, as they share several MHC molecules (i.e.: H-2K^d, H-2D^d, H- 2L^d, I-A^d, and I-E^d). As control mice we used the DBA/2J-GPNMB + strain (Jackson Lab. Strain #:007048) that has been reconstituted with the wild-type version of the *Gpnmb* gene and produces a functional protein [78]. The resulting mice were named GPNMB WT. As DBA/2J mice also lack the *C5a* gene, the BALB/c X DBA/2J-GPNMB + offsprings were selected to obtain mice lacking the *C5a* gene.

Genotypes of the offsprings were identified by Sanger sequencing using genomic DNA extracted from a small piece of ear tissue. DNA extraction was performed with NaOH (60 mM) and TRIS–HCl (1 M), followed by PCR amplification on an Eppendorf Mastercycler Nexus thermocycler, following the Jackson protocol for this strain (https://www.jax.org/Protocol?stockNumber=000671&protocolID=17636).

Primers used were:

- mGPNMB For: 5′ CCACTGAGCATTTGGAGACA 3′
- mGPNMB Rev: 5′ AGCTCCATTTCTTCCATCCA 3′
- mC5 For: 5′ TTGCTTCCACAGGTATGGTG 3′
- mC5 Rev: 5′ TTCCTCAAGGGACTGCATTT 3′

Statistical analysis

Prism software (v8.0; GraphPad Software, San Diego, CA) was used to conduct appropriate statistical procedures, as specified in figure legends. Outliers were removed using the ROUT method. A p value < 0.05 was considered significant unless noted otherwise. Overall survival time was calculated from the date of surgery to the date of death or last contact. Statistical analyses of

the results were performed using Unpaired t test with Welch's correction.

Results

Expression of GPNMB in tumors from human mesothelioma patients

In several studies, *Gpnmb* expression is significantly associated with poor prognosis in patients with cancer (e.g. breast, NSCLC, colorectal, glioma) [23, 37, 40, 54–58, 61]. However, little information has been reported in human malignant mesothelioma (MPM). From The Cancer Genome Atlas (TCGA) mesothelioma Pan-Cancer Atlas database, a series of 85 MPM patients were retrieved and analysed: higher expression of *Gpnmb* mRNA was significantly associated with lower patient survival ($p=0.019$; Fig. 1A), and the same result ($p=0.019$) was found searching for the *CD44* gene, a major GPNMB receptor and the *IL-33* gene ($p=0.045$), a cytokine that we found expressed in cancer cells downstream the engagement of CD44 [9] (Fig. 1A). We then performed correlation studies of the three genes. The Spearman correlation coefficient (r) indicated no significant association between GPNMB and CD44 or GPNMB and IL33 ($p>0.05$). The strongest correlation was observed between CD44 and IL33 ($r=0.23$, $p=0.033$), though it remains weak (Suppl. Figure 1A). Even though there seemed not to be a correlation by Cox Proportional-Hazard model, the interaction between *GPNMB* and *CD44* resulted significant (not shown). As a result, classifying patients according to combined expression of GPNMB and CD44 highlighted a significant association with a better survival in $GPNMB^{lo}/CD44^{lo}$ patients ($p=0.001$ by log-rank test) (Fig. 1B). Next, we quantified the soluble circulating levels of GPNMB in the plasma of 72 patients with a pathologically confirmed diagnosis of MPM. Compared to a cohort of 86 healthy donors, GPNMB levels were significantly higher in MPM patients ($p<0.001$), as shown in Fig. 1C.

We then investigated GPNMB expression by immunohistochemistry in 28 surgical MPM samples. Immunostaining was distinctly evaluated in tumor cells and in the inflammatory stroma. Staining with anti-CD206 was performed to identify macrophages. Figure 1D, E shows representative images of GPNMB and CD206 in two different human MPM samples, and Fig. 1F the global results of all cases examined. As expected, CD206 positivity marked the macrophage infiltrate of the stroma, while tumor cells were negative. Analysis with anti-GPNMB showed an expression pattern quite similar to that of anti-CD206, as the signal was most frequently found in the stroma (Suppl. Fig. 1B), although in 13/28 samples positivity for tumor cells was detected, mostly as a diffuse staining (Fig. 1D), suggestive of the soluble protein binding the nearby cells. To identify the nature of the GPNMB-producer cells we performed an RNAscope experiment. As shown in Fig. 1G, *Gpnmb* RNA staining (purple) and CD68 staining (brown) had a similar pattern of expression and Fig. 1H depicts the double immunostaining where it is evident that GPNMB is produced by CD68+ macrophages in human mesothelioma tissues, while cancer cells are predominantly negative. These findings indicate that in human MPM the main GPNMB-producer cells are CD68+ TAMs and not cancer cells themselves as found in several other tumor types.

We studied whether cancer cells had any role in the modulation of GPNMB production in macrophages. Indeed, we previously reported that *Gpnmb* was a top upregulated gene in tumor-cocultured macrophages [8]. Five human MPM patient-derived established cell lines were tested (CD60, CD481, CD487, CD404, CD317). Notably, none of them spontaneously produced relevant amount of GPNMB, maximum levels being 0.25 ng/mL (Suppl. Figure 1C); however, the conditioned medium from the MPM cell lines was able to stimulate GPNMB production in human monocyte-derived macrophages, with significantly higher levels compared to untreated cells (Suppl. Figure 1C). Overall, the results demonstrate that in human mesothelioma samples GPNMB is expressed by infiltrating macrophages, possibly upregulated by tumor-derived products, and that higher RNA levels in tumor tissues are associated with worse patient prognosis.

Set up of an orthotopic murine malignant mesothelioma model

To study the functional role of GPNMB in mesothelioma, we turned to a murine MPM model. Two previously characterized mouse mesothelioma cell lines were

(See figure on next page.)

Fig. 1 Expression of GPNMB in human malignant mesothelioma tissues. **A** TCGA analysis in 85 MPM patients for mRNA levels of *Gpnmb*, *CD44* and *IL-33* genes, and **B** survival of patients classified according to high/low expression of the GPNMB and CD44 genes. P value by log-rank test. **C** Plasmatic levels of soluble GPNMB measured by ELISA in 72 patients with pathologically confirmed diagnosis of MPM and in 86 healthy donors. Statistical analysis Unpaired t-test (< 0.0001). **D** Representative images of immunohistochemistry of GPNMB and **E** of CD206 in two distinct cases of human MPM. **F** heat map quantification in 28 MPM patients. **G** RNAscope experiment in two distinct cases of human MPM: single staining of *Gpnmb* RNA (purple) or CD68 (brown); double staining (**H**) is shown for each corresponding sample

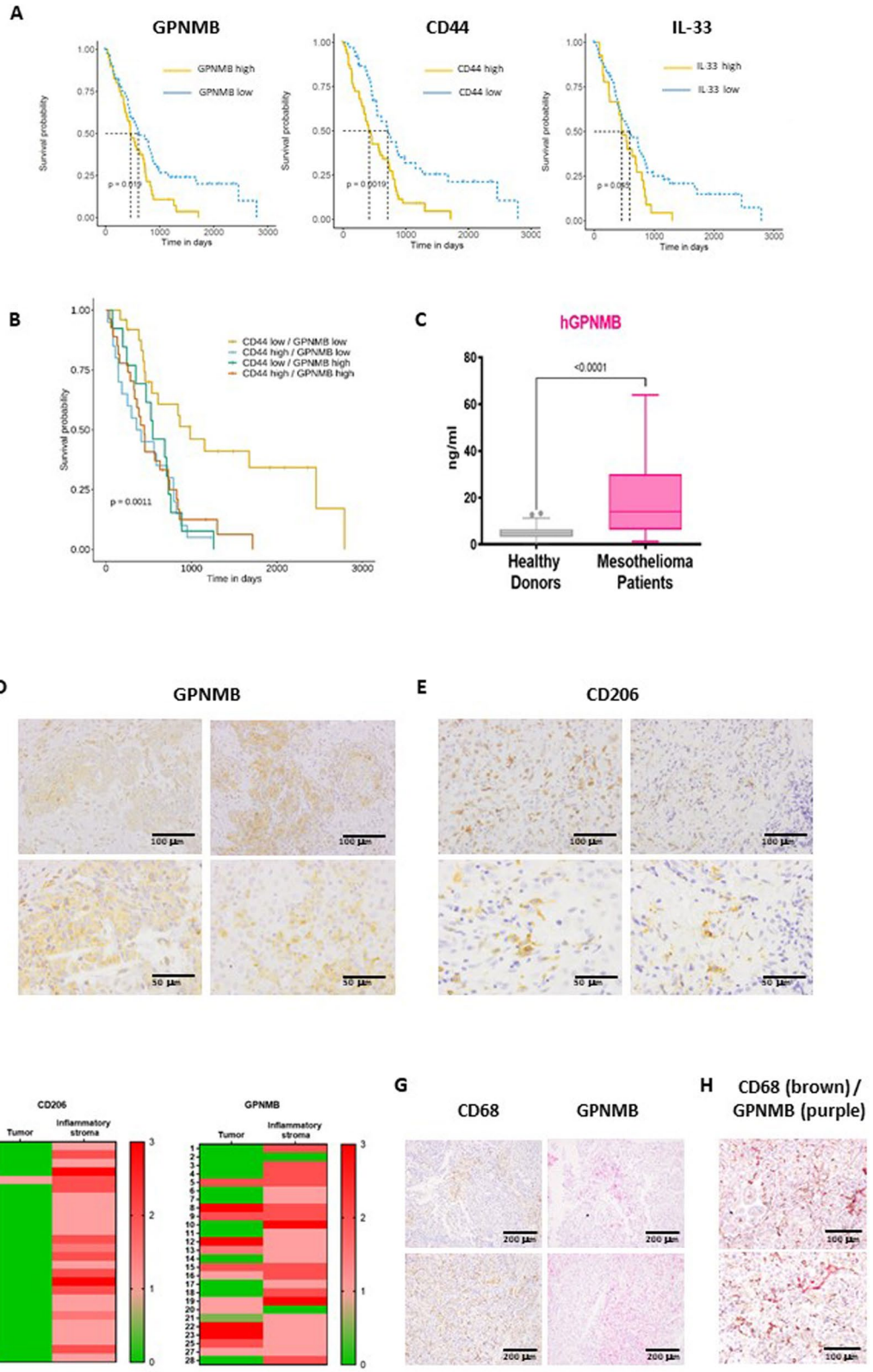

Fig. 1 (See legend on previous page.)

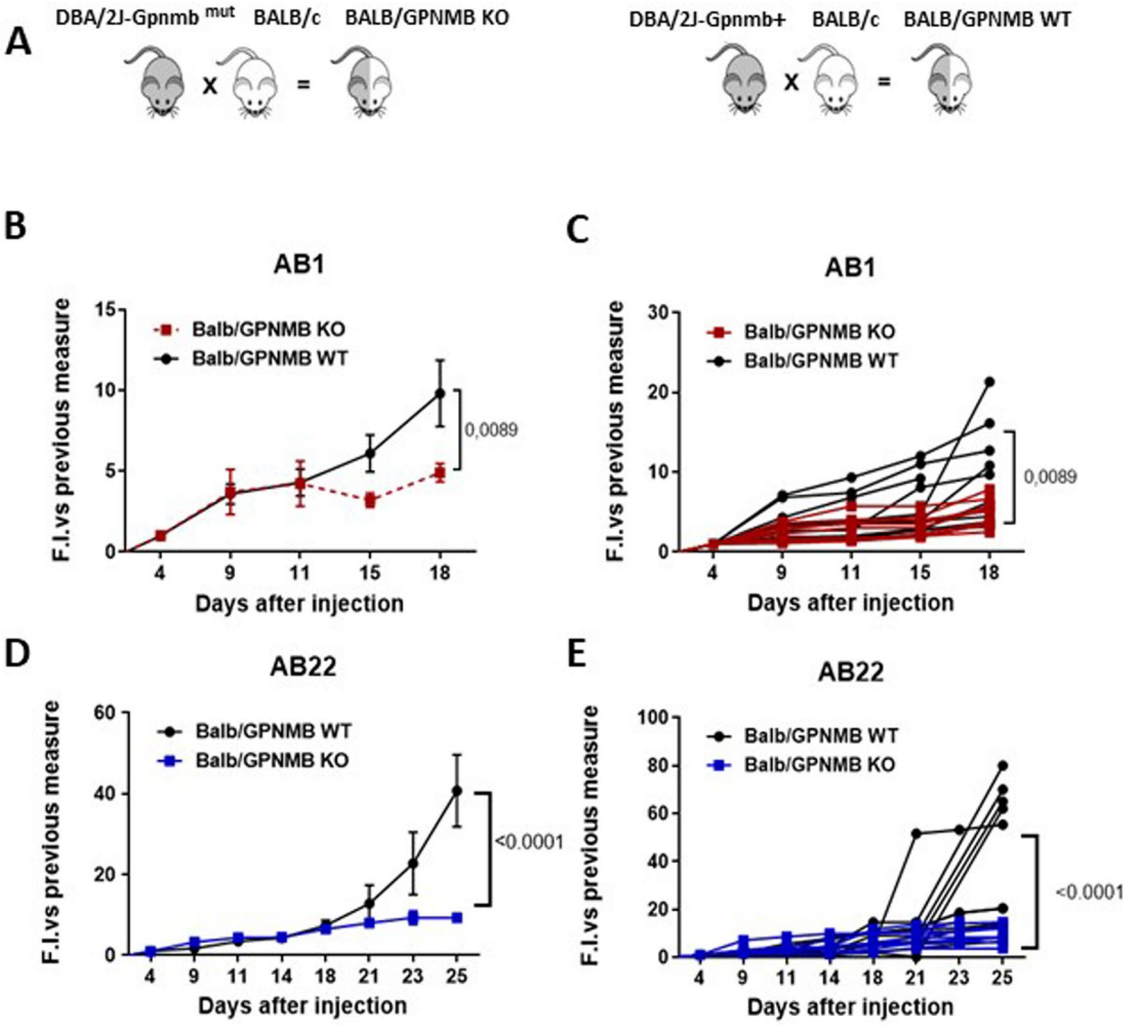

Fig. 2 Growth of murine MPM cells in DBA/2J-Gpnmb mutant mice. **A** Crossing of DBA/2J mice (GPNMB-deficient) and DBA/2J-GPNMB + mice (GPNMB-reconstituted) with BALB/c mice to generate a hybrid strain on a BALB/c background. BALB/c X DBA/2J strain (GPNMB KO) and the reconstituted strain BALB/c X DBA/2J-Gpnmb + (GPNMB WT) were used in the experiments. **B** Tumor progression (mean values of 5 mice) of AB1 cells in GPNMB KO mice (red lines) and in GPNMB WT mice (black lines), and **C** in each single mouse. Results are expressed as fold increase (F.I.) relative to the previous quantification. **D** Tumor progression (mean values of 5 mice) of AB22 cells in GPNMB KO mice (blue lines) and in GPNMB WT mice (black lines) and **E** in each single mouse. Statistical analysis Two-way ANOVA

used: AB1 and AB22 cell lines, with a sarcomatoid and epithelioid phenotype, respectively [75, 76]. We set up an intra-thoracic model of mesothelioma that nicely recapitulates the growth of human MPM (Suppl. Fig. 2A) [76]. Luciferase-expressing AB1 or AB22 cells were injected intrathoracically in syngeneic BALB/c mice and tumor growth was followed by the IVIS in vivo imaging system up to the day of sacrifice; as shown in a representative experiment (Suppl. Fig. 2B). Tumor progression can be expressed as radiance values over time (Suppl. Fig. 2C) or as fold increase of radiance values relative to the previous quantification (Suppl. Fig. 2D). Tumor burden was also verified by histological confirmation, that optimally matched (> 95%) with luminescence detection, as previously reported [76]. Tumor nodules developed along the internal surface of the pleura, further spreading and colonizing the most peripheral areas of the lungs, without forming neoplastic masses outside the thoracic cavity; a representative image of the whole lung and two magnified images of a tumor nodule are shown in Suppl. Fig. 2E. Immunohistochemistry on tumor slices showed high infiltration of Iba+ macrophages, poor infiltration of CD8 lymphocytes, the angiogenic network of CD31+ vessels and substantial negativity for cellular GPNMB, with

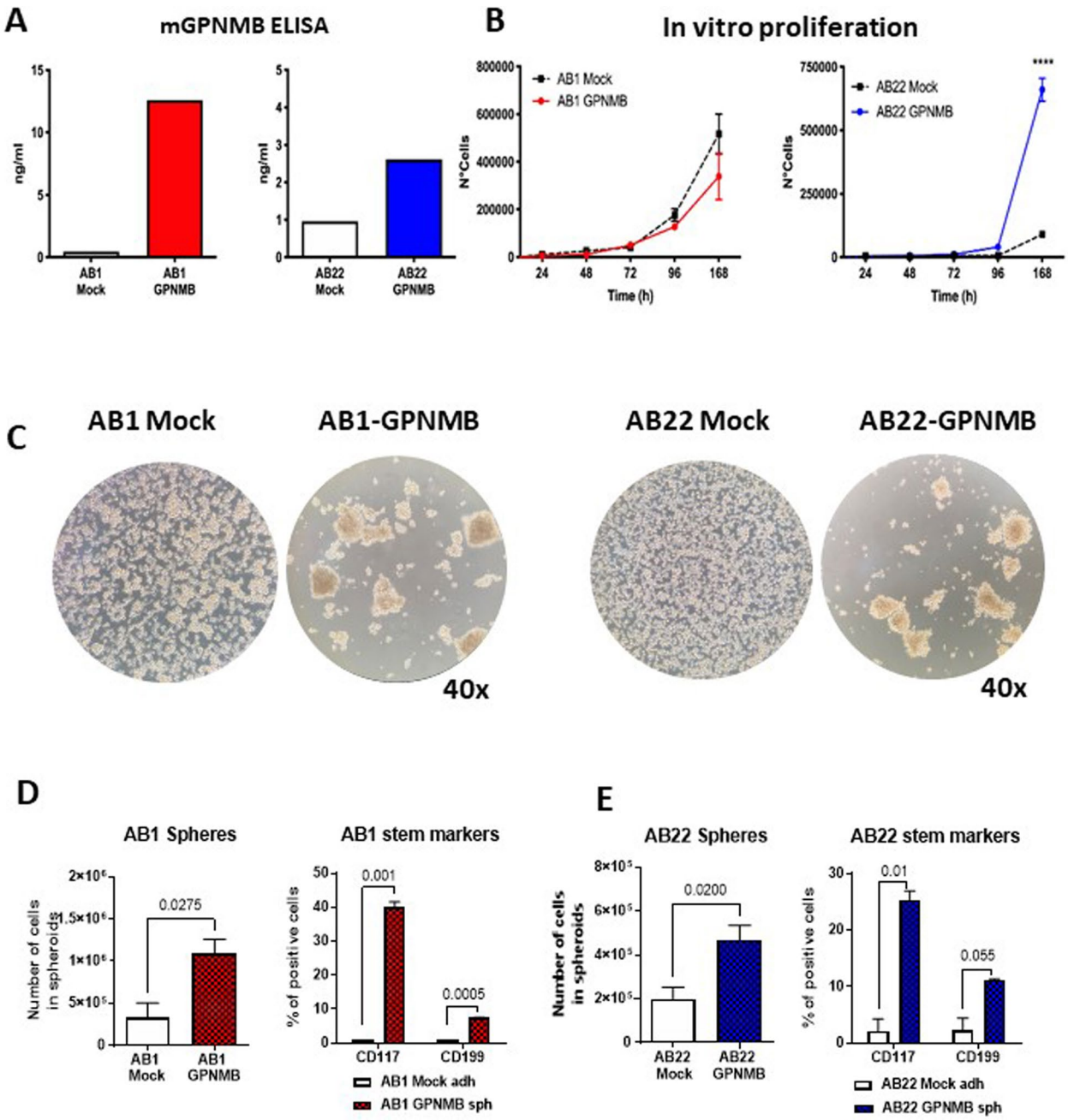

Fig. 3 Effects of GPNMB on the growth of murine MPM cells in vitro. **A** ELISA of GPNMB in Mock and GPNMB-transduced AB1 and AB22 cells. **B** In vitro proliferation of Mock and GPNMB-transduced cells. **C** In vitro sphere formation of Mock and GPNMB-transduced tumors cells from AB1 and AB22 cell lines. **D** Quantification of spheres and phenotype analysis for stem cell markers in adherent Mock-AB1 cells (adh) and in dissociated spheres from GPNMB-AB22 cells (sph). **E** Same as in **D** for AB22 cells. Statistical analysis Two-way ANOVA for B, **** $p < 0.01$, Student t-test, Welch's correction for D and E

a faint diffuse staining (Suppl. Figure 2F). Of note, once tested in vitro for soluble GPNMB production, both AB1 and AB22 cell lines produced low levels of the protein (less than 1 ng/mL). Conversely, F4/80+ TAMs in these murine tumors express GPNMB, as shown by double immunostaining (Suppl. Fig. 2G). Therefore, similarly to human MPMs, in this murine model the protein GPNMB

is not produced by cancer cells but by tumor-infiltrating macrophages.

Reduced growth of murine MPM cells in DBA/2J-Gpnmb defective mice

To investigate the role of macrophage-derived GPNMB in murine mesothelioma, we performed experiments in DBA/2J mice that lack a functional *Gpnmb* gene due to a spontaneous mutation [77]; in DBA/2J mutant mice, all cells, including macrophages, are unable to produce the mature protein. Instead, the DBA/2J-GPNMB+ strain has been reconstituted with the wild-type version of the *Gpnmb* gene and produces a functional protein [78]. As the AB1 and AB22 mesothelioma cells were generated on a BALB/c background, both DBA/2J and DBA/2J-GPNMB+ mice were crossed to obtain a hybrid BALB/c X DBA/2J strain (named GPNMB KO) and the reconstituted strain BALB/c X DBA/2J-Gpnmb+ (GPNMB WT) (Fig. 2A and scheme depicted in Suppl. Fig. 3). BALB/c and DBA/2J mice have a high level of similarity from an immunological point of view, as they share several MHC molecules (see M&M). Murine MPM cells were injected orthotopically in the thorax of GPNMB WT or GPNMB KO mice. Strikingly, both AB1 cells and AB22 cells (Fig. 2B and C) developed significantly smaller tumor masses in GPNMB-defective mice. Figure 2B shows tumor growth over time of AB1 cells as mean of 5 mice per group, while Fig. 2C shows each single mouse. Figure 2D and E shows tumor growth of AB22 cells with a similar delayed progression in GPNMB KO mice. Overall, the results indicate that host-derived GPNMB is playing a relevant role in tumor growth of murine mesothelioma in vivo.

Functional role of GPNMB in the growth of murine MPM cells

To confirm that GPNMB could be a driver of mesothelioma growth, we ectopically expressed *Gpnmb* in the murine MPM cell lines. AB1 and AB22 cells were infected with a lentiviral vector expressing the *Gpnmb* gene under the CMV promoter, together with the mCherry gene. Mock-infected cells received only the mCherry gene. mCherry positive cells were selected by FACS sorting. Validation experiments revealed that overexpression of GPNMB was successful and that transduced AB1 and AB22 cells produced 12.5 and 2.5 ng/mL, respectively, as measured in ELISA (Fig. 3A). In vitro analysis of cell proliferation showed that AB22-GPNMB cells had a striking growth increase compared to AB22-Mock cells, over a 7-day period (Fig. 3B); instead, AB1-GPNMB cells showed no evident modification in the speed of in vitro proliferation (Fig. 3B).

To explain this divergent result, we considered that other factors could possibly be involved in regulating cell proliferation. As a matter of fact, we recently reported that MPM cells produce the cytokine Osteopontin, that serves as a potent endogenous growth factor for these mesothelioma cells [79]. As AB1 cells secrete a very high amount of Osteopontin, we suspect that the lack of increased proliferation in GPNMB-transduced AB1 cells could be due to the presence of high osteopontin that may have masked the driving effect of GPNMB.

We and other reported that GPNMB is implicated in the expansion of tumor cells with features of cancer stem cells [9, 15, 50, 51]. We therefore performed an in vitro assay of sphere formation culturing AB1 and AB22 cells in Iscove's medium supplemented with growth factors (mEGF and mFGF). Only GPNMB-expressing cells were able to form self-renewing spheres. Representative pictures of Mock and GPNMB-transduced AB1 and AB22 cells in culture are shown in Fig. 3C. The phenotype analysis of the dissociated spheres demonstrated they expressed typical stemness markers such as CD117, CD199 on their cell surface (Fig. 3D and E).

We next studied the growth of GPNMB-transduced and Mock cells in vivo (Fig. 4). AB1 GPNMB-cells grew significantly faster than Mock-cells as shown in Fig. 4A as mean of 5 mice per group and in Fig. 4B for each single mouse. In vivo images are depicted in Fig. 4C. Similar findings were obtained when AB22 cells were used: GPNMB-transduced cells grew significantly more than

(See figure on next page.)

Fig. 4 Effects of GPNMB on the growth of murine MPM cells in vivo. **A** Tumor progression of AB1 GPNMB-transduced and Mock cells in vivo (mean values of 5 mice) and, **B** in each single mouse. Results are expressed as fold increase (F.I.) relative to the previous quantification. **C** In vivo imaging by IVIS. **D** Tumor progression of AB22 GPNMB-transduced and Mock cells (mean values of 5 mice) and, **E** in each single mouse. **F** in vivo imaging by IVIS. **G** Representative images of histopathology of murine lungs of mice injected with AB1 GPNMB-transduced and Mock cells, and **H** of mice injected with AB22 GPNMB-transduced and Mock cells. **I** Histopathological quantification of tumor nodules. **L** Immuno-histochemistry of tumor sections stained with H&E, anti-Iba1 (macrophages), anti-GPNMB, anti-CD31 (vessels) and anti CD8 (T lymphocytes). **M** Quantification of the tumor area positive for GPNMB. **N** Quantification of the tumor area positive for Iba1. Statistical analysis: two-way ANOVA for A, B, D, E; Student t-test Welch's correction for I ($p < 0.01$) and L ($p < 0.05$)

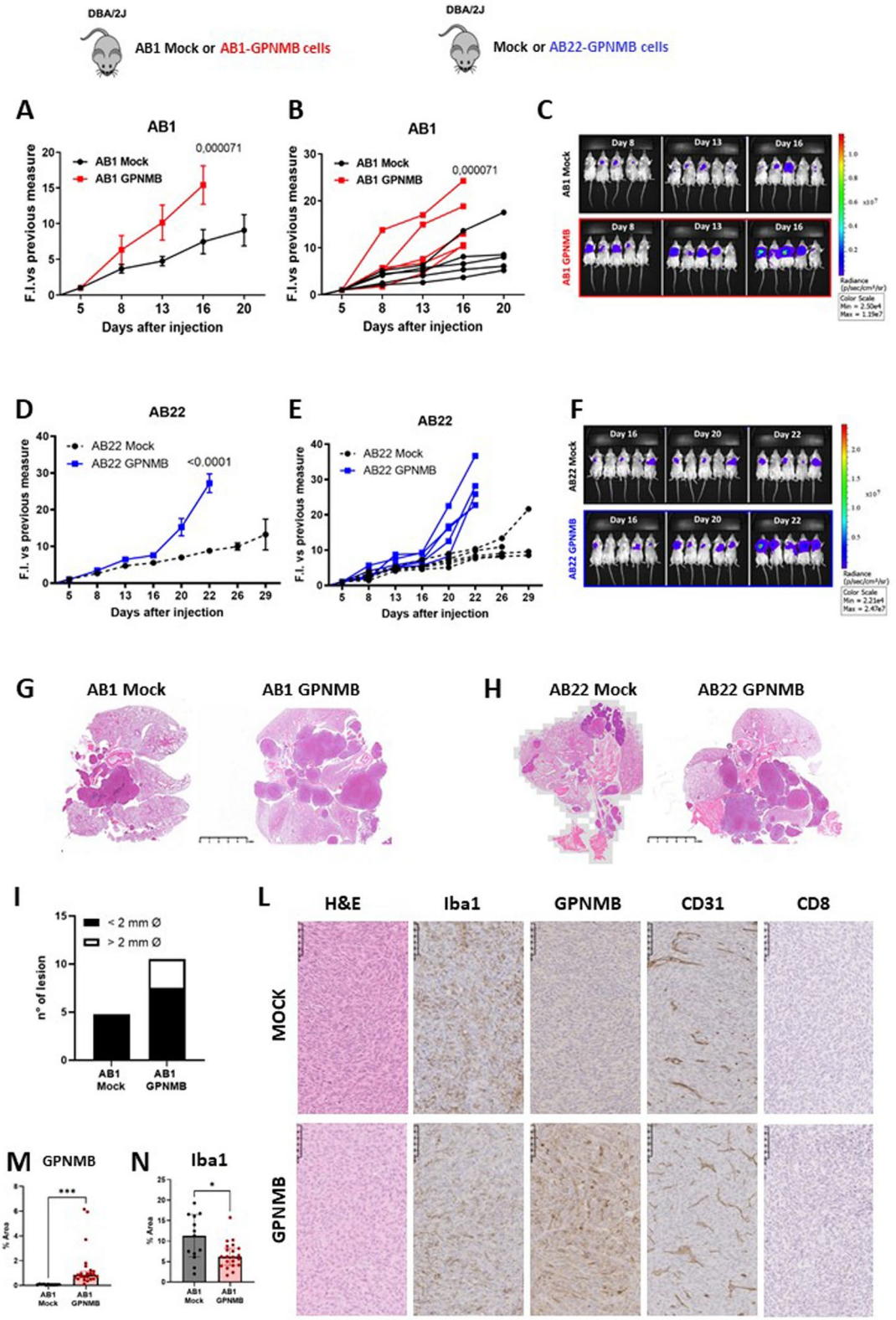

Fig. 4 (See legend on previous page.)

Mock-cells (Fig. 4D,E, and in vivo images in Fig. 4F). Histopathological images of the whole lungs show larger tumors in mice bearing GPNMB-transduced tumors (Fig. 4G and H). The number of tumor nodules was quantified by histological examination: GPNMB-expressing cells had more tumor nodules, especially of bigger size compared to those formed by Mock-cells (Fig. 4G). Immunohistochemistry of these tumors was performed to investigate the leukocyte infiltrate and to verify GPNMB expression by cancer cells. As expected, GPNMB-transduced cancer cells were strongly positive for GPNMB (Fig. 4H and I); the infiltration of Iba1 + macrophages was slightly reduced compared to Mock cells (Fig. 4H and L) while there were no substantial changes in the density of CD8+ T cells and CD31+ vessels (Fig. 4H).

Overall, these results demonstrate that the ectopic expression of GPNMB in murine mesothelioma cells is associated with faster progression of tumor growth in vivo.

Blockade of the CD44 receptor reduces tumor growth in vivo

CD44 is a major signaling receptor for GPNMB [9, 15]. To confirm the protumoral role of GPNMB, we blocked the CD44 signaling with an anti-CD44 mAb. After tumor cell injection in the thorax, mice were treated with anti-CD44 mAb (10 mg/kg) at days 8, 11, 14, 17 and 20, as detailed on top of Fig. 5. A significant reduction in tumor growth was observed in mice treated with the anti-CD44 antibody compared with mice treated with an anti-irrelevant antibody. Figure 5A, B shows the results expressed as radiance values over time as mean of 5 mice per group and in each single mouse. In Fig. 5C, D the results are calculated as F.I over the previous measurement. In vivo images by IVIS are depicted in Fig. 5E. Immunohistochemistry of tumor nodules showed that CD3+ lymphocytes and CD31+ vessels were slightly more in anti-CD44 treated tumors, while Iba + macrophages did not differ in control and treated mice; in contrast, the tumor area stained for GPNMB was significantly less in anti-CD44 treated mice (Fig. 5F).

On the whole, the results indicate that inhibition of GPNMB signaling reduces tumor growth of murine mesothelioma cells in vivo; blockade of CD44 may be considered a strategy to limit the pro-tumoral effect of GPNMB in the progression of malignant mesothelioma.

Discussion

Malignant mesotheliomas are aggressive tumors resistant to therapies, the pathogenesis of which is linked to the long-lasting chronic inflammation caused by exposure to asbestos present in inhaled air. In the context of tumor-promoting inflammation, macrophages play a predominant role and in fact the MPM leukocyte infiltrate is generally very rich in macrophages, especially with an M2-like phenotype, while T lymphocytes accumulate in the periphery and are excluded from the tumor tissue. Immunohistochemistry studies and more recent spatial transcriptomics analyses reported that the density of macrophages in MPM tissues is associated with a worse prognosis [62–64, 66, 68, 80–85].

In this study we have investigated the expression and functional role of the protein GPNMB in human and murine mesotheliomas. The TCGA analysis from MPM patients revealed that high levels of GPNMB are associated with lower patient survival. Conversely, the combined low expression of GPNMB and of CD44 was associated with better survival. The circulating levels of GPNMB in human MPM were also significantly higher than in normal subjects, however, differently from the intra-tumor mRNA, the plasmatic GPNMB levels did not reach a statistically significant difference for patient survival ($p = 0.43$, not shown). Instead, in a recent study in small cell lung cancer, high circulating levels of GPNMB were associated with poor prognosis [40].

We found in this study that TAMs in human MPM tissues—and not cancer cells—are the main producers of GPNMB, as *Gpnmb* specific RNA colocalizes with the CD68 macrophage marker. In line with this finding, several established human cell lines derived from patient surgical tumors do not produce GPNMB. We also demonstrate that coculture of monocytes/macrophages with MPM tumor cell conditioned medium induces GPNMB production and release of the soluble protein by myeloid cells. These data corroborate our previous findings on macrophages "educated" by tumor cell lines of pancreatic origin and by murine primary fibrosarcoma [8, 9]. We also previously demonstrated that cancer cells exposed

(See figure on next page.)

Fig. 5 Blockade of the CD44 receptor reduces tumor growth in vivo. Mice were treated with a neutralizing anti-CD44 mAb or an irrelevant Ab (10 mg/kg) at days 8, 11, 14, 17 and 20 post AB22 cell injection. **A** Tumor progression of AB22 cells in control and anti-CD44 treated animals (mean values of 5 mice, expressed as average radiance) and, **B** in each single mouse. **C** Results expressed as fold increase (F.I.) relative to the previous quantification (mean values of 5 mice, and **D** in each single mouse. **E** In vivo imaging by IVIS. **F** Immunohistochemistry of tumor nodules stained for the quantification of the leukocyte infiltrate and for the expression of GPNMB. Statistical analysis Mixed effect model for **A**–**D**; Student t-test Welch's correction for F (*: < 0.05; ***: (*: < 0.01))

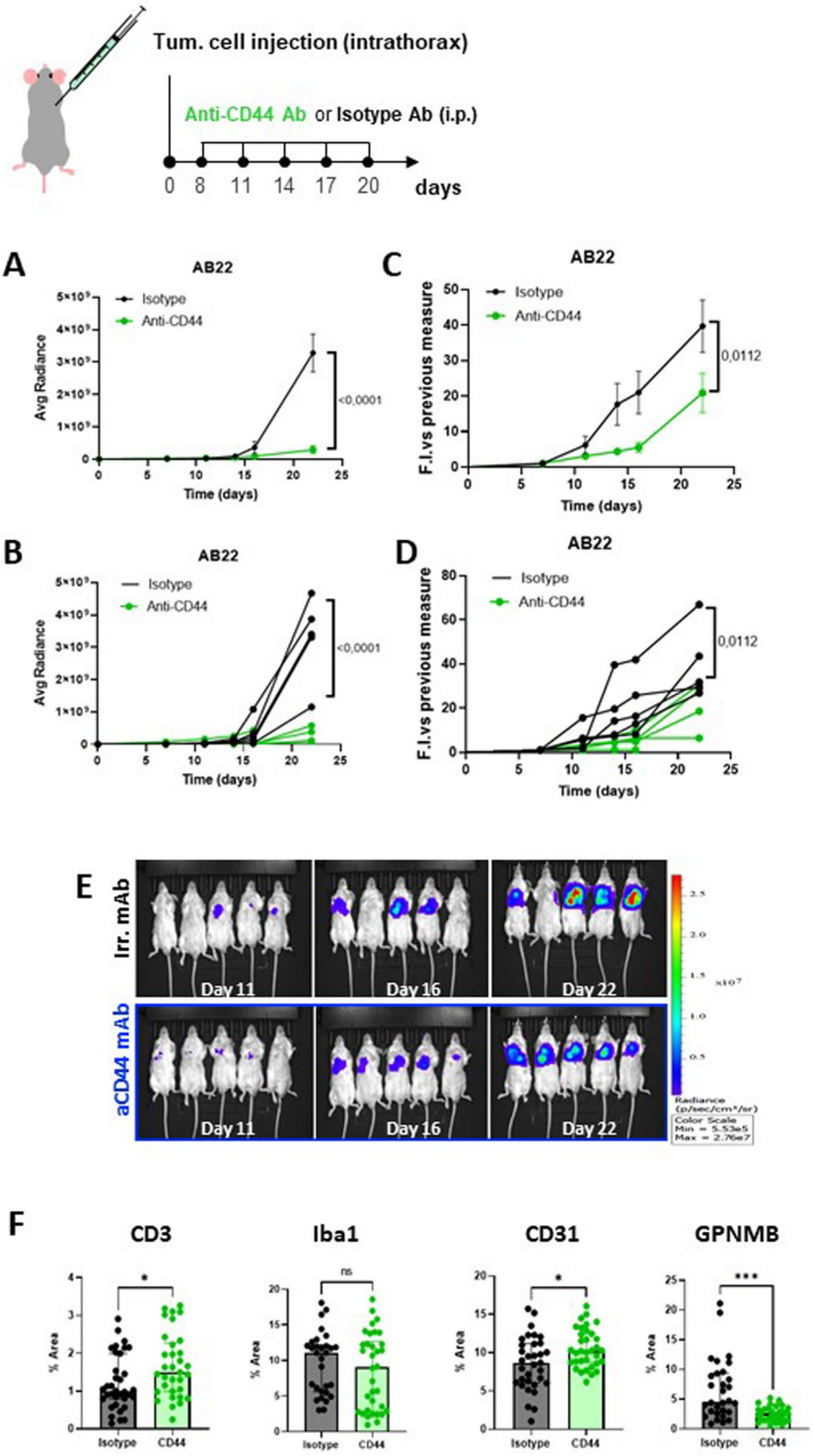

Fig. 5 (See legend on previous page.)

to macrophage-derived GPNMB or transduced with the *Gpnmb* gene, grew faster in vivo, generated more spontaneous lung metastases and strikingly expanded the pool of cancer stem cells [9]. In this study, we extend these findings to murine mesotheliomas: the ectopic expression of GPNMB significantly increases the number of cancer stem cells and GPNMB-AB1 and AB22 tumors grow remarkably more in vivo in an intra-thoracic syngeneic model. Overall, the results suggest a functional loop where tumors stimulate the production of GPNMB in macrophages and this protein, in turn, acts on tumor cells by increasing their proliferation and number of cancer stem cells. The pro-tumoral role of host-derived GPNMB appears important in vivo, as in DBA/2J-Gpnmb mutant mice—that cannot produce the protein—tumor growth is dramatically reduced.

The relevance of GPNMB-expressing macrophages in tumors received much attention in the recent years.

A number of studies have identified clusters of GPNMB+ TAMs by single cell transcriptome analysis. [5, 46, 58, 60, 61, 86].

Notably, Wu and coll. reported that small pleural/peritoneal macrophages in a mouse model of mesothelioma express GPNMB, together with other M2-like markers (TREM2, STAB1, LAIR1 and MARCO) and play a key role in promoting mesothelioma development [87]. Cortese et al. recently described a subset of TAMs in human liver metastases from colorectal cancer, expressing GPNMB and TREM2, whose high density is significantly correlated with shorter survival in patients. The transcriptome of these GPNMB + TREM2 + TAMs is enriched in pathways of matrix degradation, angiogenesis, and lipid metabolism [61]. Macrophages expressing GPNMB have been reported also in other pathological conditions, including tissue fibrosis, lipid dysregulation and accumulation of pathological aggregates, in the liver or brain. The single-cell transcriptome analyses of lipid-associated macrophages includes the expression of Gpnmb, Trem2, Cd63, Cd9 and APOE [30, 88].

Thus, a number of studies agrees that GPNMB+ macrophages also express other markers typical of the M2 polarization. In tumors, GPNMB+ TAMs have been categorized as protumoral/immunosuppressive, and their density has been associated with poor prognosis in several cancer types, overall confirming the protumoral role of GPNMB and the importance of myeloid cells producing this protein.

As MPM is a difficult to treat cancer [62–68], novel therapeutic approaches are highly necessary. Inhibition of GPNMB could be a viable option; furthermore, GPNMB has been demonstrated as a negative regulator of checkpoint blockade immunotherapy [23]. A human mAb that specifically targets GPNMB, linked to monomethyl auristatin, a potent cytotoxic compound, has been generated (Glembatumumab vedotin, CDX-011) and tested in the clinic in advanced breast, melanoma and osteosarcoma patients. Treatment with Glembatumumab vedotin was well tolerated but the efficacy results in phase II studies were disappointing and antibody production was discontinued [89–94]. The conjugated mAb Glembatumumab vedotin was designed to reach tumor cells overexpressing the transmembrane isoform of GPNMB. It is not clear if the soluble form of GPNMB cleaved by activated proteases can be efficiently blocked by this compound.

GPNMB acts on different receptors, including integrins and CD44, and activates various functional pathways. A more efficient strategy might be to block GPNMB-CD44 signaling. CD44 is a well-known target in cancer being overexpressed in various solid tumors, including MPM, and is also a marker of stem cells [95–97].

We previously reported that GPNMB binds to the CD44 receptor expressed by tumors and stimulates the production of IL-33, which functions as a growth factor for cancer stem cells [9]. It is noteworthy that our TCGA analysis in human MPM indicated that high levels of CD44 and of the downstream cytokine IL-33 are associated with worse prognosis, suggesting that the GPNMB-CD44-IL-33 pathway may be relevant in human mesothelioma. In this study we neutralized CD44 with a blocking antibody to counteract the protumoral effect of GPNMB in MPM-bearing mice and obtained a significant reduction of tumor growth in vivo. Several anti-CD44 mAbs have been developed and tested for their anti-tumor activity in preclinical and clinical studies [95, 96]. In MPM, CD44 has been shown to promote tumor invasiveness when interacting with hyaluronan [97]. Furthermore, CD44 binds also the cytokine osteopontin, that we recently demonstrated acts as an endogenous growth factor in mesothelioma cells in vitro and in vivo [79]. Therefore, based on this evidence, neutralization of CD44 and their various ligands may be pursued as a therapeutic strategy in malignant mesothelioma.

Abbreviations

MPM	Malignant pleural mesothelioma
TAMs	Tumor-associated macrophages
GPNMB	Glycoprotein non-metastatic B
TME	Tumor microenvironment

Supplementary Information

The online version contains supplementary material available at https://doi.org/10.1186/s12967-025-06407-4.

Supplementary material 1. Suppl. Fig. 1. **A** Scatterplots showing correlations between gene expression levels in Meso TCGA patients. Each plot includes a linear trend line with a shaded confidence interval. **B** Representative images of immunohistochemistry of GPNMB and CD206 in two distinct cases of human MPM tissues. **C** GPNMB ELISA in the cell-conditioned medium of different human MPM established cell lines and in the supernatants of monocytes cultured with the CM of human MPM cells lines. Statistical analysis by One Way Anova.

Supplementary material 2. Suppl. Fig. 2. Intra-thoracic murine model of malignant mesothelioma. **A** Luciferase-expressing murine mesothelioma cells injected intrathoracically in syngeneic BALB/c mice. **B** representative experiment of in vivo imaging by IVIS. **C** Quantification of tumor growth over time by results of average radiance and **D** by calculation of fold increase relative to the previous quantification. **E** Representative images of histopathology of murine lungs injected with MPM cells and of a tumor nodule. **F** immunohistochemistry of tumor sections stained with anti-Iba1, CD31, CD8and GPNMB. **G** Double immunofluorescence in tumor sections for F4/80+ macrophages and GPNMB.

Supplementary material 3. Suppl. Fig. 3.Crossing of BALB/c x DBA/2J mice to generate a mouse strain lacking the *Gpnmb* gene in a BALB/c background. **A** DBA/2J mice lacking a functional *Gpnmb* gene were crossed with BALB/c mice. The resulting offspring: BALB/c X DBA/2J mice were named GPNMB KO mice. **B** The DBA/2J-GPNMB+ strain that was reconstituted with the wild-type version of the *Gpnmb* gene and produces a functional protein, was crossed with BALB/c mice to generate the hybrid strain BALB/c X DBA/2J-GPNMB+. The resulting mice were named GPNMB WT. As DBA/2J mice also lack the *C5a* gene, the BALB/c X DBA/2J-GPNMB+ offsprings were selected to obtain mice lacking the *C5a* gene.

Acknowledgements
We would like to thank Fondazione Buzzi and AFEVA Sezione Casale Monferrato for their support. We would like to thank all patients that consented to be enrolled in the study.

Author contributions
C. Belgiovine and P. Allavena conceived this study. C. Belgiovine, E. Digifico, M. Erreni, S. Valentino performed the experiments. F. Grizzi, F, Pasqualini, L. Bertola and C.Recordati supervised the pathological examinations. P. Zucali, D. Pistillo took care of patient enrollement, treatment and sample collection. A. Putignano, L. Mannarino, V. Paleari performed statistical analysis. A. Mantovani, M, D'Incalci, F. Marchesi, P. Allavena drafted and revised the manuscript.

Funding
This research was partially supported by: MATCH study, AFEVA Sezione Casale Monferrato (Asbestos Victims); Fondazione Buzzi Unicem Onlus. The content of this article is the responsibility of the authors and does not reflect the views of these funding bodies. The publication fee for this work was covered by the Italian Ministry of Health's 'Ricerca Corrente' funding to the IRCCS Humanitas Research Hospital.

Availability of data and materials
Data available on request.

Declarations

Ethics approval and consent to participate
The methods were performed following the approved guidelines, and all experimental protocols were approved by the ethics committee of the IRCCS Humanitas Research Hospital, Rozzano (Milano), Italy.

Consent for publication
All authors contributed to the article and approved the submitted version.

Competing interests
No potential competing interests was associated with this manuscript.

Author details
[1]IRCCS Humanitas Research Hospital, Via Manzoni 56, 20089 Rozzano (Milan), Italy. [2]Department of Biomedical Sciences, Humanitas University, Pieve Emanuele, Milan, Italy. [3]Unit of Advanced Optical Microscopy, IRCCS Humanitas Research Hospital, Rozzano (MI), Italy. [4]Lab. Cancer Pharmacology, IRCCS Humanitas Research Hospital, Rozzano (MI), Italy. [5]Department of Veterinary Medicine, University of Milan, 26900 Lodi, Italy. [6]Mouse and Animal Pathology Laboratory (Maplab), Fondazione UNIMI, 20139 Milan, Italy. [7]Department Oncology, IRCCS Humanitas Research Hospital, Rozzano (MI), Italy. [8]Biobank, IRCCS Humanitas Research Hospital, Rozzano (MI), Italy. [9]William Harvey Research Institute, Queen Mary University of London, London, UK. [10]Department of Biotechnology and Translational Medicine, University of Milan, Milan, Italy. [11]Present Address: Lab. Molecular Mechanisms of Innate Immunity and Nucleic Acid Sensing, Department of Biology and Biotechnology "L. Spallanzani", Via Ferrata 9, 27100 Pavia, Italy.

Received: 15 January 2025 Accepted: 20 March 2025
Published online: 18 April 2025

References

1. Mantovani A, Marchesi F, Malesci A, Laghi L, Allavena P. Tumor-associated macrophages as treatment targets in oncology. Nat Rev Clin Oncol. 2017;14:399.
2. Mantovani A, Allavena P, Marchesi F, Garlanda C. Macrophages as tools and targets in cancer therapy. Nat Rev Drug Discov. 2022;21:799–820.
3. DeNardo DG, Ruffell B. Macrophages as regulators of tumor immunity and immunotherapy. Nat Rev Immunol. 2019;19:369.
4. Pittet MJ, Michielin O, Migliorini D. Clinical relevance of tumour-associated macrophages. Nat Rev Clin Oncol. 2022;19:402–21.
5. Kloosterman DJ, Akkari L. Macrophages at the interface of the co-evolving cancer ecosystem. Cell. 2023;186:1627–51.
6. Cassetta L, Pollard JW. A timeline of tumour-associated macrophage biology. Nat Rev Cancer. 2023;23:238–57.
7. Blériot C, Dunsmore G, Alonso-Curbelo D, Ginhoux F. A temporal perspective for tumor-associated macrophage identities and functions. Cancer Cell. 2024;42:747–58.
8. Solinas G, et al. Tumor-conditioned macrophages secrete migration-stimulating factor: a new marker for M2-polarization, influencing tumor cell motility. J Immunol Baltim Md. 2010;1950(185):642–52.
9. Liguori M, et al. The soluble glycoprotein NMB (GPNMB) produced by macrophages induces cancer stemness and metastasis via CD44 and IL-33. Cell Mol Immunol. 2021;18:711–22.
10. Kobayashi M, et al. Blocking monocytic myeloid-derived suppressor cell function via anti-DC-HIL/GPNMB antibody restores the in vitro integrity of T cells from cancer patients. Clin Cancer Res Off J Am Assoc Cancer Res. 2019;25:828–38.
11. Weterman MA, et al. nmb, a novel gene, is expressed in low-metastatic human melanoma cell lines and xenografts. Int J Cancer. 1995;60:73–81.
12. Safadi FF, et al. Cloning and characterization of osteoactivin, a novel cDNA expressed in osteoblasts. J Cell Biochem. 2001;84:12–26.
13. Shikano S, Bonkobara M, Zukas PK, Ariizumi K. Molecular cloning of a dendritic cell-associated transmembrane protein, DC-HIL, that promotes RGD-dependent adhesion of endothelial cells through recognition of heparan sulfate proteoglycans. J Biol Chem. 2001;276:8125–34.
14. Rose AAN, et al. ADAM10 releases a soluble form of the GPNMB/Osteoactivin extracellular domain with angiogenic properties. PLoS ONE. 2010;5:e12093.
15. Yu B, Sondag GR, Malcuit C, Kim M-H, Safadi FF. Macrophage-associated osteoactivin/GPNMB mediates mesenchymal stem cell survival, proliferation, and migration via a CD44-dependent mechanism. J Cell Biochem. 2016;117:1511–21.
16. Abdelmagid SM, et al. Osteoactivin, an anabolic factor that regulates osteoblast differentiation and function. Exp Cell Res. 2008;314:2334–51.
17. Yu B, Alboslemy T, Safadi F, Kim M-H. Glycoprotein nonmelanoma clone B regulates the crosstalk between macrophages and mesenchymal stem cells toward wound repair. J Invest Dermatol. 2018;138:219–27.

18. Nickl B, Qadri F, Bader M. Anti-inflammatory role of Gpnmb in adipose tissue of mice. Sci Rep. 2021;11:19614.
19. Suda M, et al. Glycoprotein nonmetastatic melanoma protein B regulates lysosomal integrity and lifespan of senescent cells. Sci Rep. 2022;12:6522.
20. Yu X, Li M, Wang C, Guan X. Glycoprotein non-metastatic melanoma protein B (GPNMB): an attractive target in atherosclerosis. Biochem Biophys Res Commun. 2024;732: 150386.
21. Ripoll VM, Irvine KM, Ravasi T, Sweet MJ, Hume DA. Gpnmb is induced in macrophages by IFN-gamma and lipopolysaccharide and acts as a feedback regulator of proinflammatory responses. J Immunol Baltim Md. 2007;1950(178):6557–66.
22. Li B, et al. The melanoma-associated transmembrane glycoprotein Gpnmb controls trafficking of cellular debris for degradation and is essential for tissue repair. FASEB J Off Publ Fed Am Soc Exp Biol. 2010;24:4767–81.
23. Chung J-S, et al. DC-HIL/Gpnmb is a negative regulator of tumor response to immune checkpoint inhibitors. Clin Cancer Res Off J Am Assoc Cancer Res. 2020;26:1449–59.
24. Lazaratos A-M, Annis MG, Siegel PM. GPNMB: a potent inducer of immunosuppression in cancer. Oncogene. 2022;41:4573–90.
25. Ramani V, Chung J-S, Ariizumi K, Cruz PD. Soluble DC-HIL/Gpnmb modulates T-lymphocyte extravasation to inflamed skin. J Invest Dermatol. 2022;142:1372-1380.e5.
26. Saade M, AraujodeSouza G, Scavone C, Kinoshita PF. The role of GPNMB in inflammation. Front Immunol. 2021. https://doi.org/10.3389/fimmu.2021.674739.
27. Sasaki F, et al. Expression of glycoprotein nonmetastatic melanoma protein B in macrophages infiltrating injured mucosa is associated with the severity of experimental colitis in mice. Mol Med Rep. 2015;12:7503–11.
28. Patel-Chamberlin M, et al. Hematopoietic growth factor inducible neurokinin-1 (Gpnmb/Osteoactivin) is a biomarker of progressive renal injury across species. Kidney Int. 2011;79:1138–48.
29. Zhou L, et al. Glycoprotein non-metastatic melanoma protein b (Gpnmb) is highly expressed in macrophages of acute injured kidney and promotes M2 macrophages polarization. Cell Immunol. 2017;316:53–60.
30. Hüttenrauch M, et al. Glycoprotein NMB: a novel Alzheimer's disease associated marker expressed in a subset of activated microglia. Acta Neuropathol Commun. 2018;6:108.
31. Murthy MN, et al. Increased brain expression of GPNMB is associated with genome wide significant risk for Parkinson's disease on chromosome 7p15.3. Neurogenetics. 2017;18:121–33.
32. Nakano Y, et al. Glycoprotein nonmetastatic melanoma protein B (GPNMB) as a novel neuroprotective factor in cerebral ischemia-reperfusion injury. Neuroscience. 2014;277:123–31.
33. Ono Y, Tsuruma K, Takata M, Shimazawa M, Hara H. Glycoprotein non-metastatic melanoma protein B extracellular fragment shows neuroprotective effects and activates the PI3K/Akt and MEK/ERK pathways via the Na+/K+-ATPase. Sci Rep. 2016;6:23241.
34. Prabata A, Ikeda K, Rahardini EP, Hirata K-I, Emoto N. GPNMB plays a protective role against obesity-related metabolic disorders by reducing macrophage inflammatory capacity. J Biol Chem. 2021;297: 101232.
35. Bianco V, Kratky D. Glycoprotein non-metastatic protein B (GPNMB): the missing link between lysosomes and obesity. Exp Clin Endocrinol Diabetes Off J Ger Soc Endocrinol Ger Diabetes Assoc. 2023;131:639–45.
36. Tsou P-S, Sawalha AH. Glycoprotein nonmetastatic melanoma protein B: a key mediator and an emerging therapeutic target in autoimmune diseases. FASEB J Off Publ Fed Am Soc Exp Biol. 2020;34:8810–23.
37. Maric G, Rose AA, Annis MG, Siegel PM. Glycoprotein non-metastatic b (GPNMB): a metastatic mediator and emerging therapeutic target in cancer. OncoTargets Ther. 2013;6:839–52.
38. Kuan C-T, et al. Glycoprotein nonmetastatic melanoma protein B, a potential molecular therapeutic target in patients with glioblastoma multiforme. Clin Cancer Res Off J Am Assoc Cancer Res. 2006;12:1970–82.
39. Taya M, Hammes SR. Glycoprotein non-metastatic melanoma protein B (GPNMB) and cancer: a novel potential therapeutic target. Steroids. 2018;133:102–7.
40. Liu Q, et al. GPNMB expression associates with inferior prognosis in patients with small cell lung cancer. J Cancer. 2024;15:2960–70.
41. Rose AAN, et al. Glycoprotein nonmetastatic B is an independent prognostic indicator of recurrence and a novel therapeutic target in breast cancer. Clin Cancer Res Off J Am Assoc Cancer Res. 2010;16:2147–56.
42. Tomihari M, Chung J-S, Akiyoshi H, Cruz PD, Ariizumi K. DC-HIL/glycoprotein Nmb promotes growth of melanoma in mice by inhibiting the activation of tumor-reactive T cells. Cancer Res. 2010;70:5778–87.
43. Maric G, et al. GPNMB augments Wnt-1 mediated breast tumor initiation and growth by enhancing PI3K/AKT/mTOR pathway signaling and β-catenin activity. Oncogene. 2019;38:5294–307.
44. Bao G, et al. Glycoprotein non-metastaticmelanoma protein B promotes glioma motility and angiogenesis through the Wnt/β-catenin signaling pathway. Exp Biol Med. 2016;241:1968–76.
45. Ono Y, et al. Glycoprotein nonmetastatic melanoma protein B (GPNMB) promotes the progression of brain glioblastoma via Na+/K+-ATPase. Biochem Biophys Res Commun. 2016;481:7–12.
46. Yalcin F, et al. Tumor associated microglia/macrophages utilize GPNMB to promote tumor growth and alter immune cell infiltration in glioma. Acta Neuropathol Commun. 2024;12:50.
47. Wang C, et al. Glycoprotein non-metastatic melanoma protein B functions with growth factor signaling to induce tumorigenesis through its serine phosphorylation. Cancer Sci. 2021;112:4187–97.
48. Arosarena OA, et al. Osteoactivin regulates head and neck squamous cell carcinoma invasion by modulating matrix metalloproteases. J Cell Physiol. 2018;233:409–21.
49. Hu X, Zhang P, Xu Z, Chen H, Xie X. GPNMB enhances bone regeneration by promoting angiogenesis and osteogenesis: potential role for tissue engineering bone. J Cell Biochem. 2013;114:2729–37.
50. Chen C, et al. Glycoprotein nmb is exposed on the surface of dormant breast cancer cells and induces stem cell-like properties. Cancer Res. 2018;78:6424–35.
51. Kawasaki Y, et al. GPNMB-positive cells in head and neck squamous cell carcinoma-their roles in cancer stemness, therapy resistance, and metastasis. Pathol Oncol Res POR. 2022;28:1610450.
52. Wang B, Wang L, Shang R, Xie L. MDSC suppresses T cell antitumor immunity in CAC via GPNMB in a MyD88-dependent manner. Cancer Med. 2024;13: e6887.
53. Meng Y, et al. GPNMB+Gal-3+ hepatic parenchymal cells promote immunosuppression and hepatocellular carcinogenesis. EMBO J. 2023;42: e114060.
54. Okita Y, et al. The transcription factor MAFK induces EMT and malignant progression of triple-negative breast cancer cells through its target GPNMB. Sci Signal. 2017;10: eaak9397.
55. Feng X, et al. High expression of GPNMB indicates an unfavorable prognosis in glioma: combination of data from the GEO and CGGA databases and validation in tissue microarray. Oncol Lett. 2020;20:2356–68.
56. Son S, et al. CCN3/NOV promotes metastasis and tumor progression via GPNMB-induced EGFR activation in triple-negative breast cancer. Cell Death Dis. 2023;14:1–16.
57. Xu X, et al. Adaptive resistance in tumors to anti-PD-1 therapy through re-immunosuppression by upregulation of GPNMB expression. Int Immunopharmacol. 2021;101: 108199.
58. Kimura T, et al. Glycoprotein nonmetastatic melanoma protein B impacts the malignant potential of bladder cancer cells through its hem-immunoreceptor tyrosine-based activation motif. Pathol Int. 2024;74:262–73.
59. Zhang Q, et al. Landscape and dynamics of single immune cells in hepatocellular carcinoma. Cell. 2019;179:829-845.e20.
60. Sun X, Liu X, Xia M, Shao Y, Zhang XD. Multicellular gene network analysis identifies a macrophage-related gene signature predictive of therapeutic response and prognosis of gliomas. J Transl Med. 2019;17:159.
61. Cortese N, et al. High-resolution analysis of mononuclear phagocytes reveals GPNMB as a prognostic marker in human colorectal liver metastasis. Cancer Immunol Res. 2023;11:405–20.
62. Yap TA, Aerts JG, Popat S, Fennell DA. Novel insights into mesothelioma biology and implications for therapy. Nat Rev Cancer. 2017;17:475–88.
63. Carbone M, et al. Mesothelioma: scientific clues for prevention, diagnosis, and therapy. CA Cancer J Clin. 2019;69:402–29.
64. Fennell DA, Dulloo S, Harber J. Immunotherapy approaches for malignant pleural mesothelioma. Nat Rev Clin Oncol. 2022;19:573–84.
65. Bueno R, et al. Comprehensive genomic analysis of malignant pleural mesothelioma identifies recurrent mutations, gene fusions and splicing alterations. Nat Genet. 2016;48:407–16.
66. Zucali PA, et al. Advances in drug treatments for mesothelioma. Expert Opin Pharmacother. 2022;23:929–46.

67. Tsao AS, Pass HI, Rimner A, Mansfield AS. New era for malignant pleural mesothelioma: updates on therapeutic options. J Clin Oncol Off J Am Soc Clin Oncol. 2022;40:681–92.
68. Occhipinti M, et al. Unleashing precision: a review of targeted approaches in pleural mesothelioma. Crit Rev Oncol Hematol. 2024;203: 104481.
69. Colaprico A, et al. TCGAbiolinks: an R/Bioconductor package for integrative analysis of TCGA data. Nucleic Acids Res. 2016;44: e71.
70. Team RC. A language and environment for statistical computing. In: R foundation for statistical computing. 2021.
71. Love MI, Huber W, Anders S. Moderated estimation of fold change and dispersion for RNA-seq data with DESeq2. Genome Biol. 2014;15:550.
72. Therneau, TM. A package for survival analysis in R. 2024.
73. Vázquez R, et al. Promising in vivo efficacy of the BET bromodomain inhibitor OTX015/MK-8628 in malignant pleural mesothelioma xenografts. Int J Cancer. 2017;140:197–207.
74. Davis MR, Manning LS, Whitaker D, Garlepp MJ, Robinson BWS. Establishment of a murine model of malignant mesothelioma. Int J Cancer. 1992;52:881–6.
75. Mezzapelle R, et al. Human malignant mesothelioma is recapitulated in immunocompetent BALB/c mice injected with murine AB cells. Sci Rep. 2016;6:22850.
76. Digifico E, et al. Optimization of a luciferase-expressing non-invasive intrapleural model of malignant mesothelioma in immunocompetent mice. Cancers. 2020;12:2136.
77. Anderson MG, et al. Mutations in genes encoding melanosomal proteins cause pigmentary glaucoma in DBA/2J mice. Nat Genet. 2002;30:81–5.
78. Howell GR, et al. Absence of glaucoma in DBA/2J mice homozygous for wild-type versions of Gpnmb and Tyrp1. BMC Genet. 2007;8:45.
79. Digifico E, et al. Important functional role of the protein osteopontin in the progression of malignant pleural mesothelioma. Front Immunol. 2023;14:1116430.
80. Marcq E, et al. Prognostic and predictive aspects of the tumor immune microenvironment and immune checkpoints in malignant pleural mesothelioma. Oncoimmunology. 2017;6: e1261241.
81. Blondy T, et al. Involvement of the M-CSF/IL-34/CSF-1R pathway in malignant pleural mesothelioma. J Immunother Cancer. 2020;8: e000182.
82. Pasello G, et al. Malignant pleural mesothelioma immune microenvironment and checkpoint expression: correlation with clinical-pathological features and intratumor heterogeneity over time. Ann Oncol Off J Eur Soc Med Oncol. 2018;29:1258–65.
83. Chatelain C, et al. Interplay between oncolytic measles virus, macrophages and cancer cells induces a proinflammatory tumor microenvironment. Oncoimmunology. 2024;13:2377830.
84. Shek D, et al. Identification and characterisation of infiltrating immune cells in malignant pleural mesothelioma using spatial transcriptomics. Methods Protoc. 2023;6:35.
85. Fiorilla I, et al. Chronic inflammation, oxidative stress and metabolic plasticity: three players driving the pro-tumorigenic microenvironment in malignant mesothelioma. Cells. 2023;12:2048.
86. Xiong A, Zhang J, Chen Y, Zhang Y, Yang F. Integrated single-cell transcriptomic analyses reveal that GPNMB-high macrophages promote PN-MES transition and impede T cell activation in GBM. EBioMedicine. 2022;83: 104239.
87. Wu L, et al. Defining and targeting tumor-associated macrophages in malignant mesothelioma. Proc Natl Acad Sci USA. 2023;120: e2210836120.
88. Fang Z, et al. Single-cell transcriptomic analysis reveals characteristic feature of macrophage reprogramming in liver Mallory-Denk bodies pathogenesis. J Transl Med. 2025;23:77.
89. Rose AAN, Biondini M, Curiel R, Siegel PM. Targeting GPNMB with glembatumumab vedotin: current developments and future opportunities for the treatment of cancer. Pharmacol Ther. 2017;179:127–41.
90. Vahdat LT, et al. Glembatumumab vedotin for patients with metastatic, gpNMB overexpressing, triple-negative breast cancer ("METRIC"): a randomized multicenter study. Npj Breast Cancer. 2021;7:1–10.
91. Yardley DA, et al. EMERGE: a randomized phase II study of the antibody-drug conjugate glembatumumab vedotin in advanced glycoprotein NMB-expressing breast cancer. J Clin Oncol Off J Am Soc Clin Oncol. 2015;33:1609–19.
92. Kopp LM, et al. Phase II trial of the glycoprotein non-metastatic B-targeted antibody-drug conjugate, glembatumumab vedotin (CDX-011), in recurrent osteosarcoma AOST1521: a report from the Children's Oncology Group. Eur J Cancer Oxf Engl. 2019;1990(121):177–83.
93. Ott PA, et al. A phase 2 study of glembatumumab vedotin, an antibody-drug conjugate targeting glycoprotein NMB, in patients with advanced melanoma. Cancer. 2019;125:1113–23.
94. Biondini M, et al. HSP90 inhibitors induce GPNMB cell-surface expression by modulating lysosomal positioning and sensitize breast cancer cells to glembatumumab vedotin. Oncogene. 2022;41:1701–17.
95. Ishikawa K, et al. Antitumor activities of anti-CD44 monoclonal antibodies in mouse xenograft models of esophageal cancer. Oncol Rep. 2024;52:1–10.
96. Mehner L-M, Munoz-Sagredo L, Sonnentag SJ, Treffert SM, Orian-Rousseau V. Targeting CD44 and other pleiotropic co-receptors as a means for broad inhibition of tumor growth and metastasis. Clin Exp Metastasis. 2024. https://doi.org/10.1007/s10585-024-10292-4.
97. Cortes-Dericks L, Schmid RA. CD44 and its ligand hyaluronan as potential biomarkers in malignant pleural mesothelioma: evidence and perspectives. Respir Res. 2017;18:58.

Publisher's Note